J. Innovative Eng. Nat. Sci., vol. 5, no. 2, pp. 534-544, 2025
http://doi.org/10.61112/jiens.1640685

Journal of Innovative Engineering and Natural Science
(Yenilikçi Mühendislik ve Doğa Bilimleri Dergisi)
https://dergipark.org.tr/en/pub/jiens

Original Paper

# Investigation of carbon black grades and multiwall carbon nanotube hybridization for the development of electrically conductive polyamide 6-based nanocomposite filaments

Müslüm Kaplan[a*]

[a]*Department of Textile Engineering, Bartin University, 74110 Bartin, Türkiye*

ARTICLE INFO

*Article history:*
Received
Received in revised form
Accepted

Available online

*Keywords:*
Carbon black
Polyamide 6
Nanomaterials
Conductive filament
Electrical conductivity
Nanocomposite filaments

ABSTRACT

The development of electrically conductive polymer filaments has gained significant attention for applications in smart textiles and flexible electronics. This study systematically investigates the influence of different carbon black (CB) grades and their hybridization with multiwall carbon nanotubes (MWCNTs) on the electrical and processing properties of polyamide 6 (PA6) based nanocomposite filaments. Three commercial CB grades were evaluated through morphological analysis, mixing energy measurements, and electrical resistivity characterization. Light microscopy analysis revealed that Vulcan XC72 exhibited superior dispersion homogeneity compared to XC MAX22 and XC615. The mixing energy calculations demonstrated that XC72 maintained consistent processing behavior, with energy requirements ranging from 25.067 J/cm³ at 1 wt% to 25.790 J/cm³ at 5 wt% loading. Electrical resistivity measurements showed significant differences in percolation behavior, with XC72 achieving 2.33E+03 ohm·cm at 13 wt%. Based on these findings, XC72 was selected for developing PA6/CB and PA6/MWCNT/CB hybrid nanocomposite filaments. While PA6/CB filaments showed insufficient conductivity, PA6/MWCNT filaments achieved 2.94E+00 ohm·cm at 10 wt%, and hybrid filaments demonstrated intermediate conductivity of 7.28E+00 ohm·cm. SEM analysis revealed the formation of interconnected networks where MWCNTs effectively bridged CB particles, explaining the enhanced conductivity of hybrid systems. This study provides crucial insights for developing cost-effective conductive polymer filaments through systematic filler selection and processing optimization.

## I. INTRODUCTION

In recent years, polymer nanocomposites have emerged as significant materials in various engineering applications due to their enhanced mechanical, thermal, and electrical properties. Polyamide 6 (PA6) based nanocomposites have attracted considerable attention due to their excellent mechanical properties and processing characteristics [1, 2]. Incorporating various nanofillers into PA6 matrices has been extensively studied, focusing on improving mechanical strength, thermal stability, and electrical conductivity [3, 4]. Recent studies have demonstrated that combining different fillers can lead to synergistic effects, enhancing both mechanical and electrical properties simultaneously [5-7].

Carbon black (CB) as a conductive filler in polymer composites has evolved significantly since its initial applications [8, 9]. Studies between 2020-2024 have shown that selecting appropriate CB grades and their effective incorporation into polymer matrices is crucial in developing materials for applications ranging from electromagnetic interference shielding to antistatic materials [10-12]. The morphology and surface characteristics of CB particles play crucial roles in determining their effectiveness as conductive fillers, with factors such as surface area and particle size distribution directly impacting the final composite properties [13-15].

*Corresponding author. Tel.: +90-378 501 1000; e-mail: mkaplan@bartin.edu.tr

The electrical conductivity of PA6/CB composites is fundamentally governed by percolation theory, which describes the formation of conductive networks within the polymer matrix [16, 17]. Recent investigations have revealed that the percolation threshold for these composites varies significantly, ranging from 1.24 vol% to 7.31 vol% depending on the processing conditions and blend compositions [18, 19]. The formation of conductive networks is mainly influenced by the dispersion quality and interfacial interactions between the CB particles and the polymer matrix [20-22].

Developing conductive polymer filaments has gained particular attention for applications in smart textiles and flexible electronics [23, 24]. Melt spinning has emerged as a preferred method for producing conductive filaments, with studies demonstrating the importance of processing parameters in achieving desired electrical and mechanical properties [25, 26]. Successfully producing conductive filaments requires careful optimization of factors such as spinning speed, drawing ratio, and thermal conditions [27, 28].

Recent advances in hybrid systems combining CB with other conductive fillers, particularly multiwall carbon nanotubes (MWCNTs), have shown promising results [29, 30]. These hybrid systems demonstrate enhanced electrical conductivity at lower total filler loadings than single-filler systems [31, 32]. The synergistic effect is attributed to forming more efficient conductive networks, where MWCNTs act as bridges between CB particles [33, 34]. Additionally, recent studies have shown that the crystallization behavior and morphological development in PA6/CB composites significantly influence both mechanical and electrical properties [35].

While previous studies have investigated PA6/CB composites, this work presents several innovative aspects that differentiate it from existing literature. It systematically compares three commercial CB grades through a novel integrated approach combining mixing energy measurements with electrical resistivity analysis. Unlike most studies on electrical conductivity, this research establishes clear correlations between processing energy requirements and the resulting conductive network formation. Additionally, this work explores the synergistic interaction between optimally selected CB grades and MWCNTs in hybrid systems, building upon but extending beyond recent findings by Kaplan et al. [15] and Nagel et al. [29]. The development of hybrid PA6/MWCNT/CB filaments with precisely controlled loading ratios represents a novel approach to achieving balanced electrical and processing properties, directly addressing a key challenge in conductive polymer filament production that has not been adequately addressed in previous research.

In this study, we investigate the influence of different CB grades on the electrical and processing properties of PA6-based nanocomposite filaments. Three commercial CB grades are evaluated through mixing energy measurements and electrical resistivity analysis. Additionally, we explore the potential of hybrid systems combining CB with MWCNTs to achieve enhanced electrical conductivity while maintaining processability. This research aims to contribute to the understanding of how CB grade selection and processing parameters influence the structural and electrical properties of conductive polymer filaments, providing valuable insights for developing advanced materials for emerging applications.

## II. EXPERIMENTAL METHOD

### *2.1. Materials*

The matrix polymer used was the PA6 Ultramid B24 N03 (BASF, Ludwigshafen, Germany), with a 1.13 g/cm$^3$ density and 220 °C melting point. PA6 was obtained as cylindrical pellets with 2.0 mm diameter and 2.5 mm length.

Three different grades of CB with varying surface areas and structures were selected to investigate their influence on electrical and processing properties. The CBs were supplied by Cabot Corporation (Alpharetta, Georgia, USA): Vulcan XC72 (moderate surface area, density: 264 kg/m³), Vulcan XC615 (high surface area, density: 315 kg/m³), and Vulcan XC MAX22 (ultra-high surface area, density: 190 kg/m³). According to the supplier data, Vulcan XC72 exhibits a pellet morphology with an average particle size of 30 nm, a specific surface area of 254 m²/g, and a 6 Ohm.cm volume resistivity. These three grades were selected based on their progressively increasing surface areas, which allows for investigation of the relationship between CB structure and composite properties.

The MWCNT NC7000, supplied by Nanocyl S.A. (Sambreville, Belgium), was selected for its high aspect ratio and excellent electrical conductivity. The MWCNTs exhibit a small rod morphology with >90% carbon purity, diameter of 9.5 nm, length of 1.5 μm, surface area of 250-300 m²/g, bulk density of 0.06 g/cm³, and volume resistivity of 0.001 Ohm.cm.

### *2.2 Sample Preparation*

The melt compounding process was performed using a conical twin screw micro-compounder Xplore 15 (Xplore Instruments BV, Sittard, Netherland) with a mixing chamber volume of 15 ml. Before compounding, PA6 pellets and CB fillers were dried in a vacuum oven at 85°C overnight. The materials were then fed into the micro-compounder, where processing was carried out at 270°C with a screw speed of 250 rpm for 15 minutes. Following the mixing stage, the composite material was extruded into strands by reducing the screw speed to 25 rpm without additional cooling. A filament drawing system was installed at the exit of the micro-compounder, and the composite material was drawn into filaments at predetermined winding speeds.

The compounded materials were processed into disc-shaped specimens (0.5 mm thickness, 60 mm diameter) using compression molding for electrical property measurements. The extrusion strands were cut into small pieces and molded using a Hidroliksan press at 270 °C, with a pre-melting phase of 2.5 minutes followed by pressing at 50 kN for 1.5 minutes. This process ensured uniform specimens with good material consolidation, enabling reliable electrical conductivity measurements of the PA6/CB nanocomposites.

### *2.2. Characterization*

The mixing energy (E), a crucial parameter influencing nanocomposites' processability and final properties, was calculated from the force measurements recorded during the melt mixing process. The force values (N) obtained from the micro-compounder were first converted to torque (τ) using Equation 1:

$$\tau = F \times r \quad (1)$$

where τ is the torque (N·m), F is the measured force (N), and r is the screw radius (m). Subsequently, the specific mixing energy per unit volume was calculated using Equation 2:

$$E = \int_0^t P dt = \int_0^t 2\pi . N . \tau dt \quad (2)$$

where E is the specific mixing energy (J/cm³), P is the power input (W), N is the mixing speed (250 rpm), t is the mixing duration (15 minutes), and τ is the average torque value (N·m) derived from initial and final force measurements. The micro-compounder volume (15 cm³) normalized the final mixing energy values to obtain specific mixing energy.

The electrical resistance measurements were performed using a two-point DC method. For filament samples, individual lengths of 100 mm were tested using an ISO-TECH IDM 63N digital multimeter (RS Components Ltd, Corby Northants, UK). Prior to measurement, the filament surfaces were gently cleaned with ethanol to remove any surface contamination. The specimens were fixed between two copper alligator clamps connected to the multimeter, ensuring consistent contact pressure for all measurements.

The electrical resistivity (ρ) of the filaments was calculated using Equation 3:

$$R_m = \rho . \frac{l}{A_{fib}} \quad (3)$$

where $R_m$ is the measured resistance (Ω), l is the distance between the measuring points (m), and $A_{fib}$ is the cross-sectional area of the filament (m²).

The macroscale dispersion of CB within the PA6 matrix was characterized using an Olympus optical microscope. Thin sections with a thickness of 5 µm were prepared from both compression-molded samples and extruded composite filaments. These sections were mounted on glass slides using Aquatex® mounting medium to ensure optimal optical clarity. The morphological features along the fiber direction were examined using a TESCAN MAIA3 XMU field emission gun scanning electron microscope (FESEM) (TESCAN, Brno, Czech Republic) for detailed morphological analysis of the filler distribution and orientation. Samples were carefully cut lengthwise under liquid nitrogen cooling to investigate the filler alignment and distribution parallel to the fiber axis. The prepared surfaces were then sputter-coated with a 60/40 gold-platinum layer to prevent charging during SEM observation.

## III. RESULTS AND DISCUSSIONS

### *3.1 Dispersion Analysis of CB Grades*

Light microscopy analysis revealed distinct differences in the dispersion behavior of the three CB grades in the PA6 matrix at 5 wt% loading, as shown in Figure 1. The Vulcan XC MAX22 sample (Fig. 1a) exhibited the largest agglomerates and most heterogeneous distribution, with visible CB clusters aligned along the flow direction. This

observation aligns with its ultra-high surface area characteristic, which can promote stronger particle-particle interactions and subsequent agglomeration.

In contrast, Vulcan XC615 (Fig. 1b) showed improved dispersion with smaller agglomerates and more uniform distribution throughout the PA6 matrix. The reduced agglomerate size indicates better compatibility with the polymer matrix and more effective dispersion during melt mixing. The Vulcan XC72 grade (Fig. 1c) demonstrated the most homogeneous dispersion among the three grades, with minimal visible agglomeration and uniform distribution of CB particles. This superior dispersion behavior of XC72 can be attributed to its moderate surface area (254 $m^2/g$) which provides an optimal balance between particle-particle and particle-polymer interactions.

The dispersion characteristics observed through light microscopy correlate well with the density values of the CB grades (XC MAX22: 190 $kg/m^3$, XC615: 315 $kg/m^3$, XC72: 264 $kg/m^3$). The intermediate density of XC72, combined with its surface area characteristics, appears to facilitate better dispersion in the PA6 matrix. These findings suggest that the selection of CB grade significantly influences the morphological development in PA6/CB composites, which in turn affects their processing behavior and final properties.

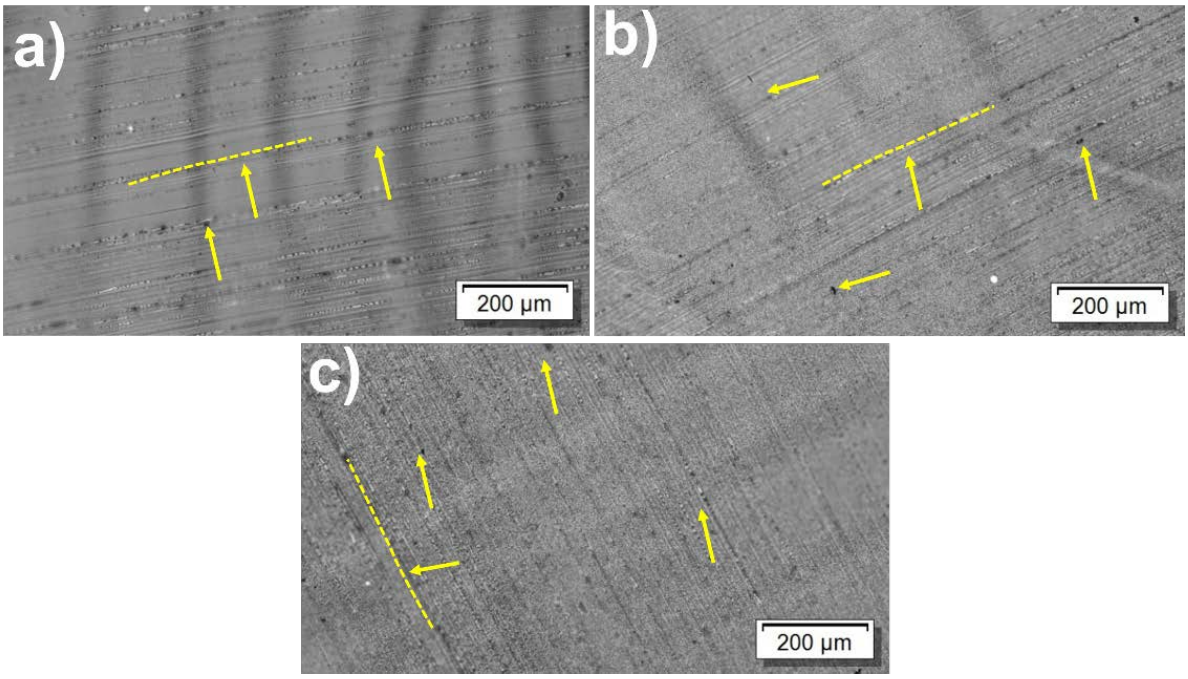


**Figure 1.** Light microscopy images of PA6/CB composites (5 wt%) with different CB grades: (a) Vulcan XC MAX22, (b) Vulcan XC615, and (c) Vulcan XC72

### *3.2 Processing Characteristics and Mixing Energy Analysis*

The impact of CB grade on the processing characteristics of PA6/CB nanocomposites was assessed through mixing energy analysis, as shown in Table 1. The mixing energy values, derived from torque measurements at 270 °C and 250 rpm, provide insight into the processability of different CB types. At 1 wt% loading, XC 615 exhibited the lowest mixing energy (23.174 $J/cm^3$), suggesting better initial dispersibility and lower resistance to flow compared to XC MAX22 (25.831 $J/cm^3$) and XC 72 (25.067 $J/cm^3$).

However, when the filler content was increased to 5 wt%, a significant increase in mixing energy was observed for XC MAX22 (31.542 J/cm³), indicating higher shear forces and potential agglomeration issues. This observation correlates well with the light microscopy results showing larger agglomerates in XC MAX22 composites. In contrast, XC 72 demonstrated the most stable processing behavior with only a minimal increase in mixing energy (25.790 J/cm³), supporting the observed homogeneous distribution in microscopy analysis.

These results suggest that while all CB grades can be processed within the selected conditions, the rheological response varies significantly with filler type and loading. The stable mixing energy of XC 72 across different loadings indicates better processability, which may be attributed to its optimal surface area and density characteristics.

**Table 1.** Mixing energy values during melt mixing process of PA6/CB nanocomposites in micro-compounder at 270 °C and 250 rpm

| Composite | Filler content (wt%) | Torque (Nm) initial | Torque (Nm) final | Average mixing energy (J/cm³) |
|---|---|---|---|---|
| PA6/ Vulcan XC MAX 22 | 1 | 20.66 | 12.23 | 25.831 |
| | 5 | 25.99 | 14.18 | 31.542 |
| PA6/ Vulcan XC 615 | 1 | 18.79 | 10.73 | 23.174 |
| | 5 | 23.51 | 14.59 | 29.912 |
| PA6 / Vulcan X C72 | 1 | 19.90 | 12.02 | 25.067 |
| | 5 | 21.19 | 11.65 | 25.790 |

*3.3 Electrical Properties of PA6/CB Composites*

The electrical resistivity values of PA6/CB nanocomposites with different CB grades and loadings are summarized in Table 2. At low CB content (1 wt%), all composites exhibited high electrical resistivity values in the range of $10^{14}$-$10^{15}$ ohm·cm, indicating typical insulating behavior. As the CB content increased to 5 wt%, XC615 showed the most significant initial decrease in resistivity (1.14E+11 ohm·cm), while XC MAX22 and XC72 maintained relatively high resistivity values.

**Table 2.** Electrical volume resistivity of polymer nanocomposites containing different CBs

| CB content (wt %) | Vulcan XC 615 | Vulcan XC 72 | Vulcan XCMAX 22 |
|---|---|---|---|
| 1.0 | 2.71E+14 | 3.11E+15 | 2.37E+15 |
| 5.0 | 1.14E+11 | 2.42E+14 | 2.04E+15 |
| 10 | 1.24E+09 | 1.14E+09 | 2.71E+05 |
| 13 | 2.60E+09 | 2.33E+03 | 6.68E+03 |

A dramatic change in electrical properties was observed at higher loadings (10-13 wt%), where both XC MAX22 and XC72 achieved substantial improvements in conductivity, reaching final resistivity values of 6.68E+03 and 2.33E+03 ohm·cm, respectively. In contrast, XC615 maintained a considerably higher resistivity of 2.60E+09 ohm·cm even at 13 wt% loading. This behavior is illustrated in Figure 2, which shows the evolution of electrical resistivity as a function of filler content for all three CB grades.

The superior conductivity achieved with XC72 at high loadings can be attributed to its optimal dispersion characteristics, as evidenced by the light microscopy analysis and supported by the stable mixing energy measurements. The formation of an efficient conductive network in XC72-based composites appears to be facilitated by its uniform distribution and moderate surface area. Conversely, the large agglomerates observed in XC MAX22 composites may explain their slightly higher resistivity despite reaching similar conductivity levels.

The poor conductivity of XC615 composites, despite their initial rapid decrease in resistivity, suggests that this grade may not form effective conductive pathways even at higher concentrations.

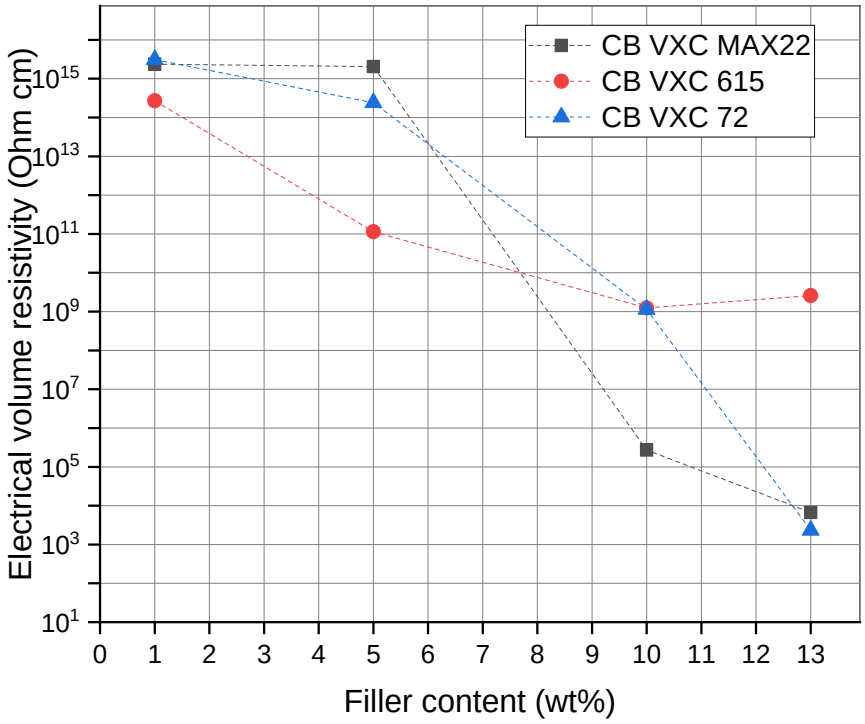


**Figure 2.** Electrical volume resistivity versus filler content for PA6 nanocomposites containing different grades of Vulcan CB (VXC MAX22, VXC 615, and VXC 72)

*3.4 Morphological and Electrical Properties of PA6/MWCNT/CB Hybrid Filaments*

The morphological features of PA6/MWCNT/CB hybrid filaments were investigated using SEM analysis, as shown in Figure 3. The longitudinal surface view of the filament (Fig. 3a) reveals distinct orientational features along the fiber axis, indicating alignment of the conductive fillers in the drawing direction. At higher magnification (Fig. 3b), the formation of interconnected conductive networks can be clearly observed, where CB particles appear to be effectively bridged by the MWCNTs. This hybrid structure, combining the large surface area of CB particles with the high aspect ratio of MWCNTs, creates continuous conductive pathways throughout the polymer matrix.

The electrical behavior of the hybrid filaments compared to pure PA6/MWCNT composites is presented in Figure 4. While PA6/CB filaments showed insufficient conductivity even at 10 wt% loading, the PA6/MWCNT filaments exhibited a characteristic percolation behavior with a sharp decrease in resistivity from 4.94E+04 ohm·cm at 2 wt% to 2.94E+00 ohm·cm at 10 wt%. The most significant reduction in resistivity occurred between 2-4 wt%, indicating the formation of an effective conductive network within the fiber structure.

The hybrid system containing equal amounts of MWCNT and CB (50:50%) showed measurable conductivity starting from 5 wt% total filler content, achieving 7.28E+00 ohm·cm at 10 wt%. Although the hybrid filaments demonstrated slightly higher resistivity values than pure MWCNT filaments at equivalent total filler loadings, their development represents a significant achievement in terms of cost-effectiveness and processability, as CB is considerably more economical than MWCNTs. The enhanced conductivity of the hybrid system can be attributed

to the synergistic effect between CB and MWCNTs, as evidenced by the SEM observations, where MWCNTs facilitate the formation of conductive bridges between CB aggregates.

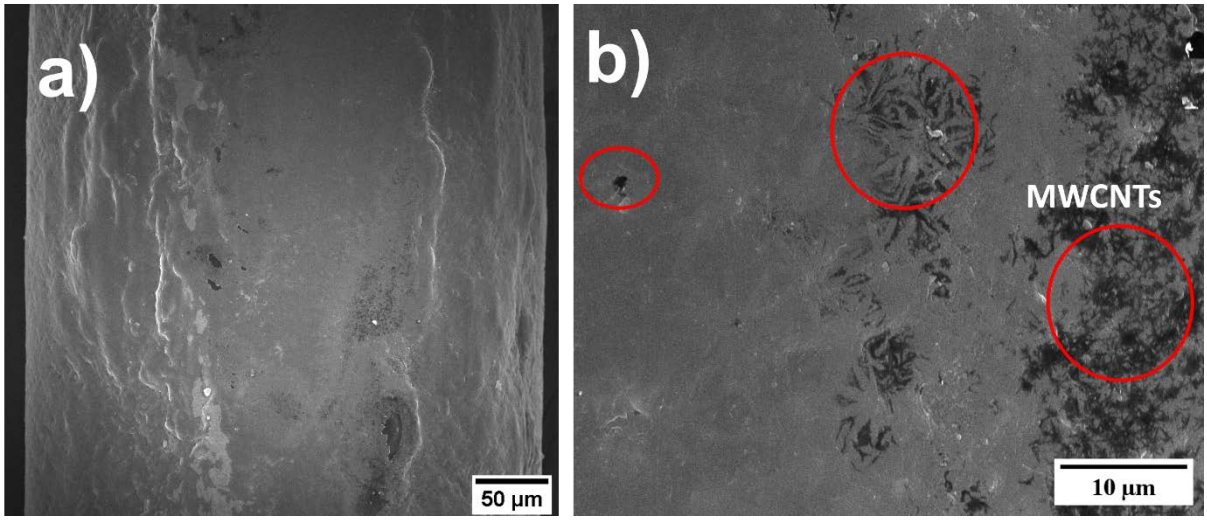


**Figure 3.** SEM micrographs of PA6/MWCNT/CB hybrid filament: (a) longitudinal surface view showing alignment along the fiber axis, and (b) higher magnification image revealing the interconnected network of CB particles and MWCNTs.

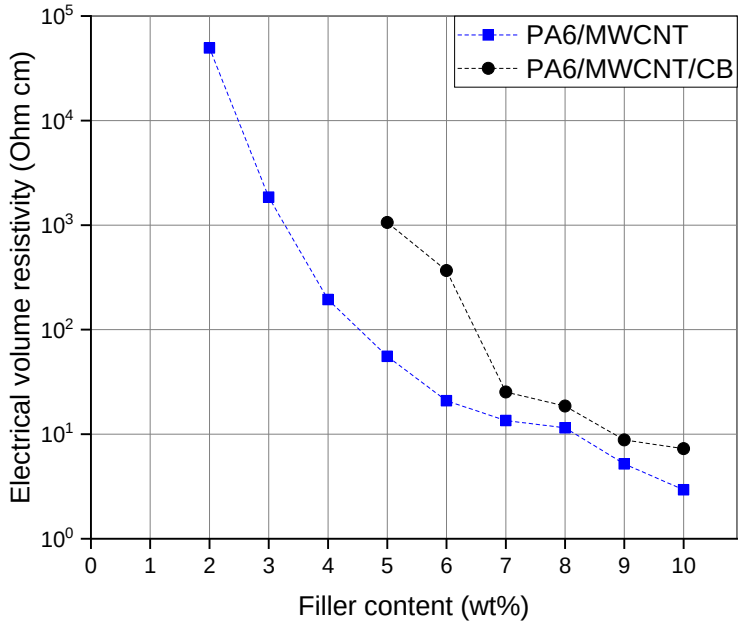


**Figure 4.** Electrical volume resistivity as a function of filler content for PA6/MWCNT and PA6/MWCNT/CB (50:50) nanocomposite filaments

Based on this comprehensive analysis, XC72 was selected as the optimal CB grade for filament production. While XCMAX22 achieved slightly lower resistivity at high loadings, XC72 offered the best balance between processing characteristics and electrical properties. Its stable mixing energy requirements across different filler contents, combined with good electrical conductivity achievement (2.33E+03 ohm·cm at 13 wt%), made it the most suitable choice for the subsequent development of both PA6/CB and PA6/MWCNT/CB hybrid nanocomposite filaments using a micro-compounder equipped with a filament drawing system.

## IV. CONCLUSIONS

The development of electrically conductive PA6-based nanocomposite filaments was systematically investigated through a comprehensive analysis of CB grade selection and filler combinations. Three different CB grades (XC MAX22, XC615, and XC72) were evaluated through light microscopy analysis, mixing energy measurements, and electrical resistivity characterization. Light microscopy revealed that XC72 provided the most homogeneous dispersion, while XC MAX22 showed larger agglomerates aligned in the flow direction. This dispersion behavior was reflected in the mixing energy requirements, where XC72 demonstrated remarkable processing stability with mixing energy values ranging from 25.067 J/cm³ at 1 wt% to 25.790 J/cm³ at 5 wt%.

The electrical resistivity measurements showed significant differences in percolation behavior among the CB grades. While XC615 exhibited an initial rapid decrease in resistivity at 5 wt% (1.14E+11 ohm·cm), both XC72 and XC MAX22 achieved superior final conductivity at 13 wt%, reaching 2.33E+03 and 6.68E+03 ohm·cm, respectively. These percolation thresholds align with findings by Li et al. [12], who reported percolation thresholds ranging from 1.24 vol% to 7.31 vol% for PA6/CB composites depending on blend composition. However, our results demonstrate that CB grade selection can significantly influence this threshold, offering a new dimension for optimization beyond what was previously investigated by Wang et al. [13] and Kaplan et al. [15].

Based on these comprehensive analyses, XC72 was identified as the optimal CB grade due to its balanced dispersion characteristics and processing stability. The subsequent development of hybrid filaments combining CB with MWCNTs demonstrated significant improvements in electrical properties. While PA6/CB filaments showed insufficient conductivity, PA6/MWCNT filaments achieved 2.94E+00 ohm·cm at 10 wt%, and hybrid filaments demonstrated intermediate conductivity of 7.28E+00 ohm·cm. This synergistic effect between MWCNTs and CB confirms observations by Chen et al. [18], who described MWCNTs acting as conductive bridges between CB particles. However, our work further quantifies this effect specifically in melt-spun filaments, an aspect not previously addressed in the literature.

SEM analysis revealed the formation of an interconnected network structure where MWCNTs effectively bridged CB particles, explaining the enhanced conductivity of the hybrid system. This morphological characteristic aligns with findings by Cheng et al. [18], who observed similar complementary effects in PA6 composites, though our study extends this understanding to fiber structures produced through melt spinning. The hybrid system's performance, while slightly less conductive than pure MWCNT composites, offers a significant cost advantage given that CB is considerably more economical than MWCNTs, addressing the economic feasibility concerns raised by Wu et al. [34].

These findings provide crucial insights for developing cost-effective conductive polymer filaments through systematic filler selection and processing optimization. The morphological analysis confirmed the importance of proper dispersion in achieving desired electrical properties, while the mixing energy measurements established processing-structure relationships. Combining multiple characterization techniques, this comprehensive approach enables a better understanding of structure-property relationships in conductive polymer composites for applications in smart textiles and flexible electronics.

**REFERENCES**


1. Gómez J, Villaro E, Karagiannidis P, Elmarakbi A (2020) Effects of chemical structure and morphology of graphene-related materials (GRMs) on melt processing and properties of GRM/polyamide-6 nanocomposites. Results Mater. https://doi.org/10.1016/j.rinma.2020.100105
2. Völtz LR, Geng S, Teleman A, Oksman K (2022) Influence of dispersion and orientation on polyamide-6 cellulose nanocomposites manufactured through liquid-assisted extrusion. Nanomaterials. https://doi.org/10.3390/nano12050818
3. LePere M (2020) Mechanical and electrical properties of 3D printed PA6 nanocomposites. NASA/SAMPE. https://doi.org/10.33599/nasampe/s.20.0255
4. Zhao M, Yi D, Yang R (2017) Enhanced mechanical properties and fire retardancy of polyamide 6 nanocomposites based on interdigitated crystalline montmorillonite–melamine cyanurate. J Appl Polym Sci https://doi.org/10.1002/app.46039
5. Brigandi PJ, Cogen JM, Wolf CA, Reffner J, Pearson RA (2015) Kinetic and thermodynamic control in conductive PP/PMMA/EAA carbon black composites. J Appl Polym Sci. https://doi.org/10.1002/app.42134
6. Sethi D, Ram R, Khastgir D (2017) Analysis of electrical and dynamic mechanical response of conductive elastomeric composites. Polym Compos. https://doi.org/10.1002/pc.24429
7. Khandavalli S, Park JH, Kariuki NN, Myers DJ, Stickel JJ, Hurst KE et al (2018) Rheological investigation on the microstructure of fuel cell catalyst inks. ACS Appl Mater Interfaces. https://doi.org/10.1021/acsami.8b15039
8. Lin G, Yu B, Hong W, Yu K, Hu Y (2020) Preparation of graded microporous layers for enhanced water management in fuel cells. J Appl Polym Sci. https://doi.org/10.1002/app.49564
9. Cheng H, Cao C, Qing-hai Z, Wang Y, Liu Y, Huang B et al (2021) Enhancement of electromagnetic interference shielding performance and wear resistance of the UHMWPE/PP blend. ACS Omega. https://doi.org/10.1021/acsomega.1c01240
10. Gao X, Huang Y, He X, Fan X, Liu Y, Xu H et al (2019) Mechanically enhanced electrical conductivity of polydimethylsiloxane-based composites. Polymers. https://doi.org/10.3390/polym11010056
11. Choi HJ, Kim MS, Ahn D, Yeo SY, Lee S (2019) Electrical percolation threshold of carbon black in a polymer matrix and its application to antistatic fibre. Sci Rep. https://doi.org/10.1038/s41598-019-42495-1
12. Li H, Tuo X, Guo B, Yu J, Guo Z (2021) Comparison of three interfacial conductive networks formed in carbon black-filled PA6/PBT blends. Polymers. https://doi.org/10.3390/polym13172926
13. Wang Y, Liu S, Zhu H, Ji H, Guo L, Wan Z et al (2021) The entangled conductive structure of CB/PA6/PP MFCs and their electromechanical properties. Polymers. https://doi.org/10.3390/polym13060961
14. Beyaz R, Ekinci A, Yurtbasi Z, Öksüz M, Ateş M, Aydın Ö (2022) Thermal, electrical and mechanical properties of carbon fiber/copper powder/carbon black reinforced hybrid polyamide 6,6 composites. High Perform Polym. https://doi.org/10.1177/09540083221114752
15. Kaplan M, Ortega J, Krooß F, Gries T (2023) Bicomponent melt spinning of polyamide 6/carbon nanotube/carbon black filaments: investigation of effect of melt mass-flow rate on electrical conductivity. J Ind Text. https://doi.org/10.1177/15280837231186174
16. Don SW, Fernando CA, Edirisinghe DG (2021) Review on carbon black and graphite derivatives-based natural rubber composites. Adv Technol. https://doi.org/10.31357/ait.v1i1.4857
17. Mei X, Zhao Y, Jiang H, Gao T, Huang ZX, Qu J (2023) Multifunctional starch/carbon nanotube composites with segregated structure. J Appl Polym Sci. https://doi.org/10.1002/app.53904
18. Chen Y, Yang Q, Huang Y, Liao X, Niu Y (2016) Synergistic effect of multiwalled carbon nanotubes and carbon black on rheological behaviors and electrical conductivity of hybrid polypropylene nanocomposites. Polym Compos. https://doi.org/10.1002/pc.24141
19. Kaplan M, Krause B, Pötschke P (2022) Polymer/CNT composites and filaments for smart textiles: melt mixing of composites. SSP. https://doi.org/10.4028/p-3g2wph
20. Grellmann H, Bruns M, Lohse F, Kruppke I, Nocke A, Cherif C (2021) Development of an elastic, electrically conductive coating for TPU filaments. Materials. https://doi.org/10.3390/ma14237158
21. Kim NS (2020) 3D-printed conductive carbon-infused thermoplastic polyurethane. Polymers. https://doi.org/10.3390/polym12061224
22. Liu W, Chang YC, Zhang J, Liu H (2022) Wet-spun side-by-side electrically conductive composite fibers. ACS Appl Electron Mater. https://doi.org/10.1021/acsaelm.2c00150
23. Dinh D, Ninh H, Nguyen H, Nguyen D, Nguyen G, Nguyen T et al (2024) Polyamide 6/carbon fibre composite: an investigation of carbon fibre modifying pathways for improving mechanical properties. Plast Rubber Compos. https://doi.org/10.1177/14658011241253553
24. Nga P, Hua P, Ngo Q, Ha T, Nguyen V, Thành N et al (2024) The effect of carbon black percentage on mechanical properties and microstructure of PA6/CB blends. East-Eur J Enterp Technol. https://doi.org/10.15587/1729-4061.2024.299067

25. Wang Z, Wang L, Meng Y, Wen Y, Pei J (2023) Effects of conductive carbon black on thermal and electrical properties of composites. J Renew Mater. https://doi.org/10.32604/jrm.2023.025497
26. Zhang J, Hong X, Long J, Liang B (2023) Preparation of ionic liquid modified graphene and its effect on enhancing the properties of PA6 composites. Polym Compos. https://doi.org/10.1002/pc.28026
27. Moronkeji O, Das D, Lee S, Chang K, Chasiotis I (2023) Local electrical conductivity of carbon black/PDMS nanocomposites subjected to large deformations. J Compos Mater. https://doi.org/10.1177/00219983231156253
28. Hamester M, Pietezak D, Dalmolin C, Becker D (2021) Influence of crystallinity and chain interactions on the electrical properties of polyamides/carbon nanotubes nanocomposites. J Appl Polym Sci. https://doi.org/10.1002/app.50817
29. Nagel J, Hanemann T, Rapp B, Finnah G (2022) Enhanced PTC effect in polyamide/carbon black composites. Materials. https://doi.org/10.3390/ma15155400
30. Hussain K, Shergill R, Hamzah H, Yeoman M, Patel B (2023) Exploring different carbon allotrope thermoplastic composites for electrochemical sensing. ChemRxiv. https://doi.org/10.26434/chemrxiv-2022-l6xb3-v2
31. Zhai W, Zhu J, Wang Z, Zhao Y, Zhan P, Wang S et al (2022) Stretchable, sensitive strain sensors for wearable electronic skins. ACS Appl Mater Interfaces. https://doi.org/10.1021/acsami.1c18233
32. Zhang H, Zhang B, Wang W, Guo Z, Yu J (2021) Highly efficient electrically conductive networks in polymer blends. J Appl Polym Sci. https://doi.org/10.1002/app.45877
33. Raju A, Das M, Dash B, Dey P, Nair S, Naskar K (2022) Variation of air permeability in rubber composites: influence of filler particle structure. Polym Eng Sci. https://doi.org/10.1002/pen.25879
34. Wu Z, Xie L, Shao Y, Wang J, Zhang M, Du J (2024) Percolation behavior and sensing performance of polypropylene-based conductive polymer composites. J Polym Sci. https://doi.org/10.1002/pol.20230894
35. Beyaz R, Ekinci A, Yurtbasi Z, Öksüz M, Ateş M, Aydın Ö (2022) Thermal, electrical and mechanical properties of hybrid polyamide composites. High Perform Polym. https://doi.org/10.1177/09540083221114752